# Similarities and Differences between Cobalamins and Cobaloximes. Accurate Structural Determination of Methylcobalamin and of LiCl- and KCl-Containing Cyanocobalamins by Synchrotron Radiation

**Lucio Randaccio,*,† Michela Furlan,† Silvano Geremia,† Miroslav Šlouf,‡ Ivana Srnova,§ and Daniele Toffoli†**

Dipartimento di Scienze Chimiche, University of Trieste, 34127 Trieste, Italy, and Departments of Inorganic Chemistry and of Physical and Macromolecular Chemistry, Charles University, Prague, Czech Republic

*Received February 7, 2000*

The accurate crystal structure determinations of MeCbl (**1**), CNCbl·2LiCl (**2**), and CNCbl·KCl (**3**), based on synchrotron diffraction data collected at 100 K and using high-quality single crystals, are reported. Refinements gave R1 indices of 0.0834 (**1**), 0.0434 (**2**), and 0.0773 (**3**). The influence of the water of crystallization and ion content on the crystal packing of these and other cobalamins (XCbl) is discussed, and a relationship between the crystal packing and the corrin side chain conformations is presented. An analysis of the bond lengths within the corrin moiety, based on 13 accurate structures with several X groups, shows that the trend of the C−C and C−N distances can be interpreted in terms of electronic and steric factors. The variation in structural, NMR and IR spectroscopic, and electrochemical properties are compared with those of cobaloximes, the $B_{12}$ model, when X is varied. This comparison indicates that the $\pi$-back-donation from metal to the CN axial ligand and the transmission of the trans influence of the X ligand are more effective in cobalamins than in cobaloximes. These findings are consistent with a significantly greater availability of electron charge on Co in cobalamins, and, hence, a semiquantitative evaluation of the electronic difference between the cobalt centers in the two systems is allowed.

## Introduction

Since the exciting work of D. Hodgkin et al., which established the structure of vitamin $B_{12}$,[1] and the subsequent elucidation of that of the coenzyme $B_{12}$ in 1968,[2] a limited number of compounds belonging to the vitamin $B_{12}$ group (X-cobalamins, XCbl) (Chart 1) were structurally characterized prior to 1980. Available structures were reviewed in 1982, together with those of the simple $B_{12}$ model, namely, cobaloximes, XCo-$(DH)_2$L, where DH = monoanion of dimethylglyoxime and L = neutral ligand.[3] Since then, several additional structures have been reported, including that of methylcobalamin, MeCbl, the other biologically important cobalamin, [4] but they have generally been of low accuracy. This has hampered a deep analysis of some important features of the Co coordination sphere, such as cis and trans influences, and the establishment of basic relationships between structure and chemical properties, as revealed in cobaloximes.[5] Although these studies on cobaloximes have furnished useful information about the factors affecting the biologically important Co−C bond homolysis in the coenzyme $B_{12}$ (AdoCbl),[6] it was not clear if the structural findings and their relationships to chemical properties in models also apply to cobalamins. Furthermore, with the increasing interest in molecular mechanics calculations[7] and theoretical calculations[8] on such systems, aimed at obtaining insight into the behavior of $B_{12}$ coenzyme, it is desirable to obtain geometrical parameters as accurately as possible.

Only few years ago, thanks to the use of synchrotron radiation, was the highly accurate structure of $(H_2OCbl)ClO_4$ ($B_{12a}$) finally reported.[9] However, a few years later the structure of the corresponding $[H_2O\text{-}10\text{-}ClCbl]ClO_4$, based on conventional source data, was determined with a similar accurancy.[10] These results suggest that improvement in the crystallization techniques is another important factor to be considered in order to obtain accurate structural data. Recent attempts[11] to obtain

† University of Trieste.
‡ Department of Inorganic Chemistry, Charles University.
§ Department of Physical and Macromolecular Chemistry, Charles University.

(1) Hodgkin, D. C.; Lindsey, J.; Sparks, R. A.; Trueblood, K. N.; White, J. G. *Proc. R. Soc.* **1962**, *A266*, 494. Brink-Shomaker, C.; Cruickshank, D. W. J., Hodgkin, D. C.; Kamper, M. J.; Pilling, D. *Proc. R. Soc.* **1964**, *A278*, 1 and references therein.
(2) Lenhert, P. G. *Proc. R. Soc.* **1968**, *A303*, 45.
(3) Glusker, J. P. In *$B_{12}$*; Dolphin, D., Ed.; Wiley: New York, 1982; Vol. 1, p 23.
(4) Rossi, M.; Glusker, J. P.; Randaccio, L.; Summers, M. F.; Toscano, P. J.; Marzilli, L. G. *J. Am. Chem. Soc.* **1985**, *107*, 1729.
(5) Bresciani-Pahor, N.; Forcolin, M.; Marzilli, Randaccio, L.; Summers, M. F.; Toscano, J. P. *Coord. Chem. Rev.* **1985**, *63*, 1. Randaccio, L.; Bresciani-Pahor, N.; Zangrando, E.; Marzilli, L. G. *Chem. Soc. Rev.* **1989**, *18*, 225. Randaccio, L. *Comments Inorg. Chem.* **1999**, *21*, 327.
(6) *Vitamin $B_{12}$ and $B_{12}$-Proteins*; Kräutler, B., Arigoni, D., Golding, B. T., Eds.; Wiley-VCH: Weinheim, 1998. *Chemistry and Biochemistry of $B_{12}$*; Banerjee, R., Ed.; J. Wiley & Sons: New York, 1999. Pratt, J. M. In *Metal Ions in Biological Systems*; Sigel, H., Sigel, A., Eds.; Marcel Dekker Inc.: New York, 1993; Vol. 29, p 229. Marzilli, L. In *Bioinorganic Catalysis*; Reedijk, J., Bouwman, E., Eds.; Marcel Dekker: New York, 1999; p 423.
(7) Marques, H. M.; Warden, C.; Hicks, R. P.; Brown, K. L. *J. Chem. Soc.* **1996**, 27. Marques, H. M.; Brown, K. L. *J. Mol. Struct.* **1995**, *340*, 97. Marques, H. M.; Hicks, R. P.; Brown, K. L. *Chem. Commun. (Cambridge)* **1996**, 1427 and references therein.
(8) Hansen, L. M.; Derecskei-Kovacs, A.; Marynick, D. S. *J. Mol. Struct.* **1998**, *431*, 53 and references therein.
(9) Kratky, C.; Färber, G.; Gruber, K.; Deuter, Z.; Nolting, H. F.; Konrat, R.; Kräutler, B. *J. Am. Chem. Soc.* **1995**, *117*, 4654.
(10) Brown, K. L.; Cheng, S.; Zubkowski, J. D.; Valente, E. J.; Kropton, L.; Marques, H. M. *Inorg. Chem.* **1997**, *36*, 3666.

10.1021/ic0001199 CCC: $19.00 
Published on Web 07/06/2000

**Chart 1**

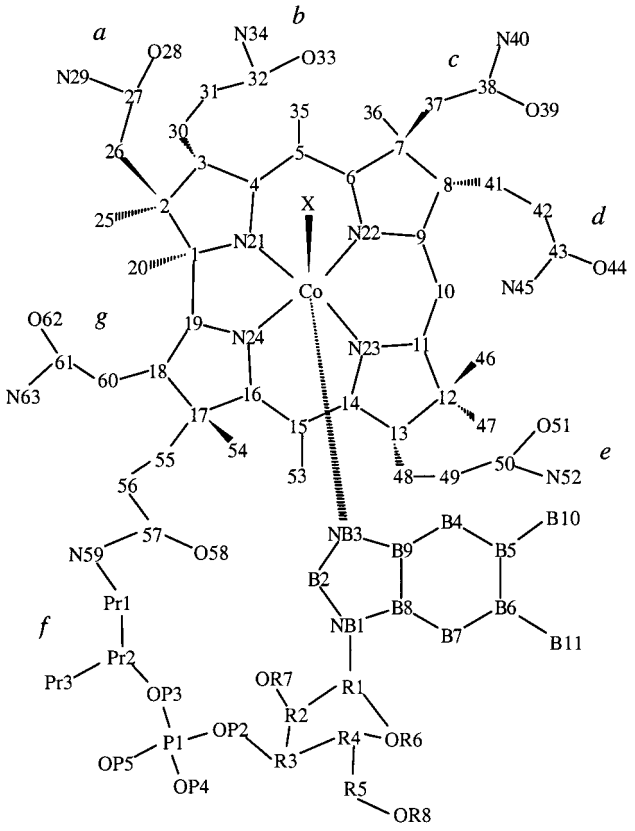


X = Me (**1**, **4**), CN (2LiCl, **2**; KCl, **3**; **5**)

high-quality single crystals of $N_3$Cbl and ClCbl were successful by using the hanging-drop method, normally used for proteins, with in situ preparation of the above derivatives starting from $(H_2O$Cbl$)$Cl. The analysis of the crystal structures, based on synchrotron diffraction data collected at 100 K, allowed a very accurate molecular geometry to be obtained. Furthermore, this study revealed that the crystals of both cobalamins contain two LiCl units per cobalt atom,[11] allowing a structural picture of the interactions of the corrin side chains with $Cl^-$ anion and $Li^+$ cations. The high crystallinity of these compounds was principally ascribed to these interactions, which decrease the conformational disorder of the flexible corrin side chains and favor the ordering of the water molecules. Preliminary results[12] indicated that crystals of composition XCbl·MCl (X = $NO_2$, CN; M= Na, K) can be obtained by the same method. More recently, the accurate structural analysis of $(SO_3$Cbl$)(NH_4)$ was also reported,[13] which allowed an estimate of the geometry of the axial fragment in thiolate cobalamins, not yet experimentally determined. This should be relevant for the other biologically important members of the $B_{12}$ group, the methylcobalamin (MeCbl), whose enzyme, methionine synthase, catalyzes the conversion of homocysteine to methionine,[14a] and the coenzyme $B_{12}$ itself of some ribonucleotide reductases.[14b]

Another biologically important aspect is connected with the understanding of the role played, at the molecular level, by the interactions of the solvent water molecules with biomolecules, which depends in part on the availability of accurate structural data. This aspect has been deeply investigated by Savage et al. in the case of the coenzyme $B_{12}$ (AdoCbl), using neutron and X-ray diffraction data.[15]

Finally, the first structural characterizations of the $B_{12}$ enzymes, methylmalonyl-CoA mutase[16a] and methionine synthase,[16b] indicates that Co is not coordinated by the 5,6-dimethylbenzimidazole residue, but is instead coordinated by a histidine residue of the protein chain. That not only the axial Co−C bond properties but also those of the axial Co−N bond are involved in the enormous enhancement of the homolysis rate was previously suggested by studies on simple models.[5,6] However, very recently the crystal structure analysis of diol dehydratase, in complex with CNCbl, the substrate, and potassium ions, has shown that the cobalamin is bound to the protein in the base-on form, i.e., the benzimidazole residue is coordinated to Co.[17a] Furthermore, this study confirms early work,[17b] which suggested that the $K^+$ ions play an essential role in the catalysis of this enzyme as well as in the binding of the $B_{12}$ coenzyme to the apoenzyme. Therefore, the hypotheses that emerged from previous work concerning the Co−C homolytic cleavage require verification, in view of the structural findings on the $B_{12}$-dependent enzymes.[16,17] All these points suggest that it is highly desirable to have accurate structural determinations of vitamin $B_{12}$ and of its biologically active derivatives. Here we report the preparation and the crystal structure analysis of MeCbl (**1**), CNCbl·2LiCl (**2**), and CNCbl·KCl (**3**), based on synchrotron data collected at 100 K. Comparison of available accurate structural data of the axial fragment in cobalamins and in cobaloximes is presented. Similarities and differences between the two systems are evidenced and discussed.

## Experimental Section

**Crystallizations.** Commercial high-purity MeCbl was obtained from Sigma, and CNCbl (stated purity by the manufacturer was greater than 98%) was obtained from Fluka. The other reactants were reagent grade and used without further purification. The complexes were crystallized as outlined below, the single crystals being grown by the hanging-drop method of vapor diffusion.

**1.** Two microliters of MeCbl aqueous solution at 25 mg/mL were mixed with 2 $\mu$L of the precipitant solution containing KF. Single crystals were obtained with typical ranges for precipitants of 10−20% in PEG400 (10% in PEG6000) and 0.5−0.30 M in KF. The prismatic single crystal, used in the final data collection, was obtained with 10% PEG400 and 0.30M KF. Attempts without PEG (with or without LiCl) were unsuccessful.

(11) Randaccio, L.; Geremia, S.; Furlan, M.; Slouf, M. *Inorg. Chem.* **1998**, *37*, 5390.
(12) Furlan, M., Ph.D. Thesis, University of Trieste, 1999.
(13) Randaccio, L.; Geremia, S.; Nardin, G.; Slouf, M.; Srnova, I. *Inorg. Chem.* **1999**, *38*, 4087.
(14) (a) Mattews, R. G.; Drummond, J. T. *Chem. Rev.* **1990**, *90*, 1275. Drennan, C. L.; Dixon, M. M.; Hoover, D. M.; Jarret, J. T.; Goulding, C. W.; Matthews, R. G.; Ludwig, M. L. In *Vitamin $B_{12}$ and $B_{12}$-Proteins*; Kräutler, B., Arigoni, D., Golding, B. T., Eds.; Wiley-VCH: Weinheim, 1998; p 133. (b) Stubbe, J.; Licht, S.; Gerfen, G.; Booker, S. In *Vitamin $B_{12}$ and $B_{12}$-Proteins*; Kräutler, B., Arigoni, D., Golding, B. T., Eds.; Wiley-VCH: Weinheim, 1998; p 320 and references therein.
(15) Bouquiere, J. P.; Finney, J. L.; Savage H. F. J. *Acta Crystallogr.* **1994**, *B50*, 566. Bouquiere, J. P.; Finney, J. L.; Lehmann, M. S.; Lindley, P. F.; Savage H. F. J. *Acta Crystallogr.* **1993**, *B49*, 79. Savage, H. F. J. *Biophys.* **1986**, *50*, 947, 967. Savage, H. F. J.; Finney, J. L. *Nature* **1986**, *322*, 717.
(16) (a) Mancia, F.; Keep. N. H.; Nakagawa, A.; Leadlay, P. F.; McSweeney, S.; Rasmusssen, B.; Boske, P.; Diat, O.; Evans, P. R. *Structure* **1996**, *4*, 339. Mancia, F.; Evans, P. R. *Structure* **1998**, *6*, 771. (b), Drennan, C. L.; Huang, S.; Drummond, J. T.; Matthews, R. G.; Ludwig, M. L. *Science* **1994**, *266*, 1669. Dixon, M.; Huang, S.; Mattews, R. G. *Structure* **1996**, *4*, 1263.
(17) (a) Shibata, N.; Mesuda, J.; Tobimatsu, T.; Toraya, T.; Suto, K.; Morimoto, Y.; Yasuoka, N. *Structure* **1999**, *7*, 997. (b) Toraya, T.; Sugimoto, Y.; Tamao, Y.; Shimizu, S.; Fukui, S. *Biochemistry* **1971**, *10*, 3475.

**Table 1.** Crystal Data and Structure Refinement Details for **1**, **2**, and **3**

| | **1** | **2** | **3** |
|---|---|---|---|
| formula | $C_{63}H_{127.2}CoN_{13}O_{32.1}$ P | $C_{63}H_{108.4}Cl_2CoLi_2N_{14}O_{24.2}P$ | $C_{63}H_{109.2}ClCoKN_{14}O_{24.6}P$ |
| fw | 1670.48 | 1623.92 | 1620.89 |
| *T*, K | 100(2) | 100(2) | 100(2) |
| $\lambda$, Å | 0.8 | 0.8 | 0.8 |
| cryst syst, space group | orthorhombic, $P2_12_12_1$ | orthorhombic, $P2_12_12_1$ | orthorhombic, $P2_12_12_1$ |
| *a*, Å | 17.280(5) | 15.360(1) | 16.015(5) |
| *b*, Å | 17.740(5) | 22.493(1) | 21.146(5) |
| *c*, Å | 32.370(5) | 23.830(1) | 23.843(5) |
| *V*, Å$^3$ | 9923(4) | 8233.1(7) | 8075(4) |
| *Z*; $D_{calcd}$, Mg/m$^3$ | 4, 1.118 | 4, 1.310 | 4, 1.333 |
| $\mu$, cm$^{-1}$ | 0.263 | 0.371 | 0.397 |
| cryst size, mm | 0.2 × 0.3 × 0.1 | 0.3 × 0.2 × 0.2 | 0.2 × 0.3 × 0.2 |
| *R* [$I > 2\sigma(I)$][a] | R1 = 0.0834, wR2 = 0.2312 | R1 = 0.0435, wR2 = 0.1244 | R1 = 0.0733, wR2 = 0.1973 |
| *R* (all data)[a] | R1 = 0.0898, wR2 = 0.2398 | R1 = 0.0438, wR2 = 0.1247 | R1 = 0.0951, wR2 = 0.2111 |

[a] $R1 = \Sigma||F_o| - |F_c||/\Sigma|F_o|$, $wR2 = [\Sigma w(F_o^2 - F_c^2)^2/\Sigma w(F_o^2)^2]^{1/2}$.

**2:** Two microliters of saturated aqueous solution of CNCbl were mixed with 2 $\mu$L of the precipitant solution containing LiCl in the range 2.0−3.5 M and PEG400 in the range 15%-27%. The used single crystal was obtained with 3.0 M LiCl and 22% PEG.

**3.** Two microliters of saturated aqueous solution of CNCbl was mixed with 2 $\mu$L of the precipitant solution containing 2.0 M KCl and PEG2000 in the range 5%-22%. The prismatic single crystal, used for data collection, was obtained with 19% PEG. Attempts with PEG400 in the range 20−50% and with PEG6000 in the range 5−22% were unsuccessful.

**X-ray Structural Determinations.** The diffraction experiments were carried out at the X-ray diffraction beamline of the Elettra Synchrotron, Trieste (Italy), using the rotating-crystal method. Data were collected on a 345 mm MAR image plate with crystals mounted in loop and frozen to 100 K using a nitrogen stream cryocooler. Crystallographic data for **1**−**3** are given in Table 1. The diffraction data were integrated using the DENZO program,[18] and reflections were subsequently scaled and merged using the SCALEPACK program.[18] Friedel equivalent reflections were not merged, and no absorption correction was applied. The structure of **1** was refined starting from the atomic parameters of the previous X-ray analysis.[4] The phase problem for **2** and **3** was solved using as a starting model the coordinates of an isomorphous structure. The structural parameters were refined by full-matrix least-squares on $F^2$ for all data using SHELXL-97.[19] Final *R* factors and refinement details are reported in Table 1.

## Results

**Preparation of the Crystals.** Several attempts to prepare single crystals of MeCbl, containing alkaline halides, failed, and free-ion red crystals of MeCbl (**1**) were always obtained. X-ray data collections with several crystals of **1** were performed and analyzed. The best data set was chosen for the present analysis. On the contrary, high-quality deep red crystals of CNCbl·2LiCl (**2**), isomorphous with those of XCbl·2LiCl (X = Cl, $N_3$), were obtained in the presence of LiCl.

By addition of the suitable reactant NaX (X = $NO_2$, $N_3$) to ($H_2O$Cbl)Cl in the presence of MCl (M = Na, K),[12] deep red single crystals of apparent composition XCbl·MCl grew, but unfortunately they were of low quality. However, when CNCbl was crystallized in the presence of KCl, good-quality crystals of CNCbl·KCl (**3**) were obtained. Therefore, on the basis of the above results it may be concluded that, at the present time, inclusion of electrolytes occurs only for "inorganic" cobalamins, with X = monoanionic ligand or cyanide.

**Crystal Packing of 1, 2, and 3.** The crystal packings of **1**−**3**, viewed along the crystallographic *a* axis, are shown in Figures 1a, 2, and 3, respectively. It has been shown[13,20] that the crystal packing of isomorphous cobalamins can be distinguished in four groups (clusters), according to the *c*/*a* and *b*/*a* ratios of the unit cell parameters. Isostructural compounds belong to the same cluster. MeCbl and $(H_2O$Cbl$)^+$ cannot be assigned to any of these clusters. Cyanocobalamins **2** and **3** belong to clusters IV and I, respectively**.** The crystal packings for all the clusters are similar. In fact, the cobalamin molecules are arranged in such a way as to form large cavities, running along the *a* axis, where solvent molecules, ions, and host molecules are located. The shape of the cavity in clusters I, II, and IV[12,13,20] is similar and differs somewhat from that accurately analyzed in III.[15] Each cavity can be described as being made of a central channel running along a crystallographic 2-fold screw axis (parallel to *a*) and connected to side pockets, at intervals defined by the symmetry of that axis. An ordered scheme of H-bonded water molecules and ions (when present) characterizes the pockets. The channel is characterized by a disordered pattern of solvent molecules with fractional occupancy.[12,13,21] The crystal packing of MeCbl exhibits a completely different arrangement and does not differ significantly from that previously described in MeCbl·acetone (**4**).[4] This is clearly apparent when Figures 1−3 are compared. The large channels in **1** run along the crystallographic *a* axis (at $z = 0$ and 0.5) as shown in Figure 1b. In **1**, the different orientation of the corrin moiety with respect to the *a* axis results in the formation of cavities appreciably larger than those found in clusters I and IV. This is evident from comparison of the volume per cobalamin molecule, which have a similar size in clusters I−IV (AdoCbl is appreciably larger than the other cobalamins). In fact, this volume is 2480, 2050, and 2019 Å$^3$ for **1**, **2**, and **3**, respectively. Typical values of that volume at low temperature for the other clusters are 2230 (II, CNCbl·acetone (wet) at 88 K (**5**))[22] and 2279 Å$^3$ (III, AdoCbl at 12 K[15]).

The proposed H-bond scheme for **1**, involving amide chains and water molecules with full occupancy, is given in Table 2. Analysis of the H-bond pattern does not seem to confirm the intramolecular H-bond between N59 and OP3 found in the less accurate determination of **4**, unless a distorted bifurcated H-bond between N59, OP3, and OW2 is assumed. In fact, the N59−H···OP3 angle is 80° against that of 166° for the N59−

(18) Otwinowski, Z.; Minor, W. *Methods Enzymol.* **1996**, *276*, 307.
(19) Sheldrick, G. M. *SHELXL-97*; Universität Göttingen: Göttingen, 1997.
(20) Gruber, K.; Jogl, G.; Klintsher, G.; Kratky, C. In *Vitamin $B_{12}$ and $B_{12}$-Proteins*; Kräutler, B., Arigoni, D., Golding, B. T., Eds.; Wiley-VCH: Weinheim, 1998; p 335.
(21) Wagner, T.; Afshar, C. E.; Carell, H. L.; Glusker, J. P.; Englert, U.; Hogekamp, H. P. C. *Inorg. Chem.* **1999**, *38*, 1784.
(22) Kräutler, B.; Konrat, R.; Stupperich, E.; Färber, G.; Gruber, K.; Kratky, C. *Inorg. Chem.* **1994**, *33*, 4128.

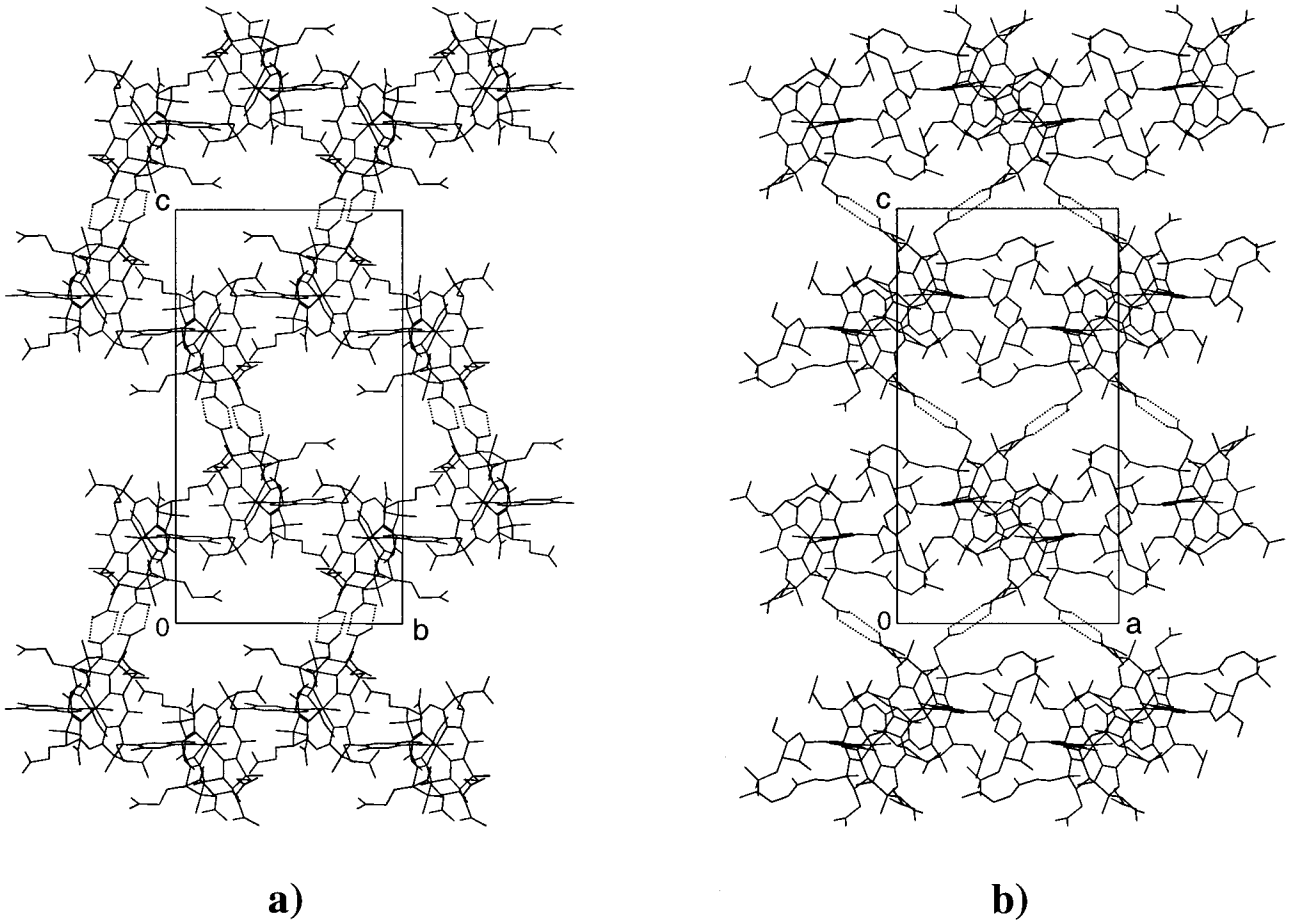


**Figure 1.** Crystal packing of the cobalamin molecules of **1** viewed along the cystallographic axes *x* (a) and *y* (b). For the sake of clarity, the content of the cavity is not shown.

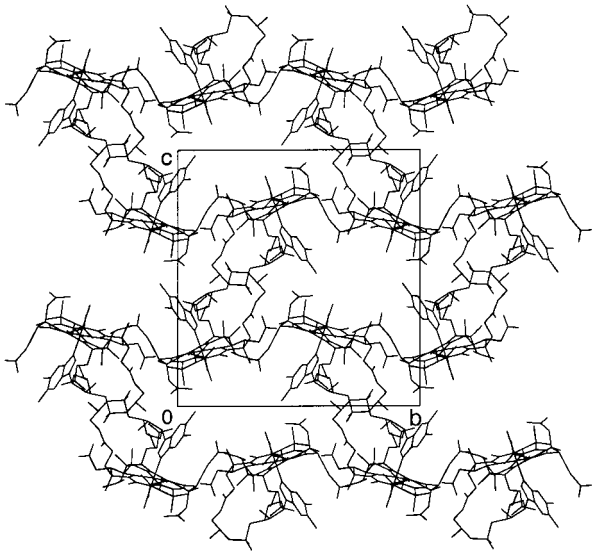


**Figure 2.** Crystal packing of the cobalamin molecules of **2** viewed along the cystallographic *x* axis. For the sake of clarity, the content of the cavity is not shown.

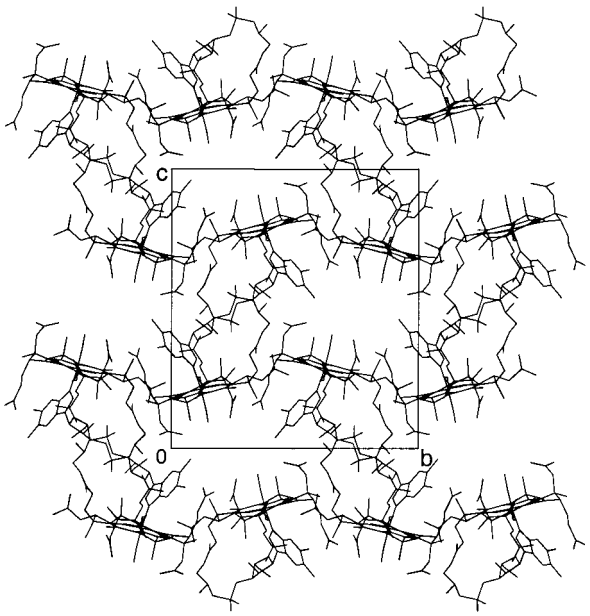


**Figure 3.** Crystal packing of the cobalamin molecules of **3** viewed along the cystallographic *x* axis. For the sake of clarity, the content of the cavity is not shown.

H···OW2 H-bond (see discussion). Analogously, the proposed H-bond between OR7 and OP2 in **4** should be ruled out in **1** because of the very narrow CR2−OR7···OP2 angle of 63°. Therefore, it is more likely that OR7 donates a H-bond to OW2 (OW5 in **4**), with a CR2−OR7···OW2 angle of 115°. Such an assignment is consistent with that proposed in **2** (see below). The OW2 molecule donates two H-bonds to OW5 and OW3, which in turn donates a H-bond to OP5 (Table 2). The H-bonding interactions within the nucleotide loop in **1** are depicted in Chart 2a. The remaining side chains are also involved in H-bonds with water molecules. In **1**, the O and $NH_2$

**Table 2.** H-Bond Scheme within the Pocket of **1**, **2,** and **3**

| H-donor | | H-acceptor | |
|---|---|---|---|
| | **1**[b] | | |
| OW1 | | | O51 (2.752(7) Å), *OW10*[I] (2.59(1) Å) |
| OW2 | OR7 (2.741(6) Å), N59 (2.993(8) Å) | | OW3 (2.816(1) Å), OW5 (2.746(1) Å) |
| OW3 | OW2, *OW19*[I] (2.60(1) Å) | | OP5 (2.74(1) Å),*OW12*[I] (2.68(2) Å), *OW13*[I] 2.69(3) Å) |
| OW4 | *OW15*[II] (2.79(1) Å) | | O28 (2.74(1) Å), OP5[III] (2.770(9) Å) |
| OW5 | OW2 | | O62 (2.70(1) Å), *OW27*[IV] (2.67(3) Å) |
| OW6 | N40[V] (2.880(4) Å) | | O51 (2.841(7) Å), OP4[VI] (2.780(7) Å) |
| OW7 | N45 (2.96(3) Å) | | O44 (2.94(1) Å), OP4[VII] (2.67(1) Å) |
| OW8 | N40 (2.99(1) Å) | | O58[VIII] (3.10(1) Å), *OW28*[VIII] (3.27(4) Å) |
| OW9 | OR8[VI] (2.80(1) Å) | | *OW21*[IV] (2.86(2) Å), *OW24*[I] (2.92(1) Å) |
| O28 | OW4, N63[II] (3.21(1) Å) | N29 | O62[II] (2.847(7) Å), *OW26* (3.08(2) Å) |
| O33 | *OW17*[IX] (2.99(1) Å) | N34 | *OW15*[II] (2.78(4) Å) |
| O39 | *OW16* (2.70(1) Å) | N40 | OW6[VIII], OW8 |
| O44 | OW7,*OW26*[VIII] (2.66(1) Å) | N45 | OW7 |
| O51 | OW1, OW6 | N52 | OP5[VI] (2.829(9) Å), *OW14*[X] (3.00(2) Å) |
| O58 | OW8[V], OW10[IV] (2.84(1) Å) | N59 | OW2 |
| O62 | OW5, N29[IV] | N63 | O28[IV], *OW12* (3.28(2) Å), *OW13* (2.80(3) Å) |
| OP4 | OW6[VII], OW7[VI] | OR7 | OW2 |
| OP5 | OW3, OW4[XI], N52[VII] | OR8 | OW9[VII] |
| | **2**[c] | | |
| OW1 | **Li2 (1.977(8) Å)** | | O58[I] (2.838(4) Å), OW3[II] (2.807(4) Å) |
| OW2 | OR7[III] (2.720(4) Å), N59[III] (3.133(4) Å) | | OW3[III] (2.924(4) Å), OP4 (2.773(4) Å) |
| OW3 | OW1[III] (2.807(4) Å),OW2[II] | | O33[III] (2.796(4) Å), OP5 (2.696(4) Å) |
| OW4 | **Li1 (1.932(6) Å)** | | O33[IV] (2.779(4) Å), Cl2[V] (3.179(3) Å) |
| OW5 | N63[III] (2.966(5) Å), **Li1 (2.026(7) Å)** | | O39[VI] (2.727(4) Å), Cl2[V] (3.154(4) Å) |
| O28 | **Li2 (1.920(7) Å)** | N29 | O44[VII] (3.270(5) Å), Cl1 (3.248(5) Å) |
| O33 | OW4[I], OW3[II] | N34 | Cl1[VIII] (3.200(3) Å) |
| O39 | OW5[IX] | N40 | *OW13* (3.07(1) Å), *OW16* (2.96(1) Å), N (3.132(5) Å) |
| O44 | N29[VIII], *OW8* (2.82(1) Å), **Li2**[VIII] **(1.951(7) Å)** | N45 | *OW10* (2.94(1) Å), *OW12* (2.82(1) Å), *OW15* (3.15(1) Å) |
| O51 | OR8 (2.897(4) Å), **Li2**[IV] **(1.937(7) Å)** | N52 | Cl2 (3.360(4) Å), *OW8*[X] (3.04(1) Å) |
| O58 | OW1[IV] | N59 | OW2[II] |
| O62 | **Li1**[II] **(1.923(7) Å)** | N63 | Cl1 (3.213(4) Å), OW5[II] |
| OP4 | OW2, **Li1 (1.886(7) Å)** | OR7 | OW2[II] |
| OP5 | OW3 | OR8 | O51 |
| Cl1 | N29, N34[VII], N63, *OW6*[X] (3.32(1) **Å**), *OW7* (2.90(1) Å) | | |
| Cl2 | OW4[XI], OW5[XI], N52, *OW11* (3.02(1) Å), *OW14*[XI] (3.22(1) Å) | | |
| | **3**[d] | | |
| OW1 | N52[I] (2.92(2) Å) | | O58[I] (2.768(9) Å), OW2 (2.812(9) Å) |
| OW2 | OW1 | | OP5 (2.674(7) Å), OW3 (2.890(8) Å) |
| OW3 | OW2, OR7 (2.764(7) Å) | | Cl (3.28(1) Å), OP4[I] (2.712(8) Å) |
| OW4 | *OW6*[II] (2.78(1) Å), *OW6A*[II] (3.12(1) Å) | | O44 (2.89(1) Å) |
| OW7 | N29[III] (3.06(1) Å), N45[IV] (2.953(5) Å) | | *OW5*[V] (2.423(5) Å) |
| O28 | N45[VI] (2.902(9) Å), N52[VII] (3.13(1) Å) | N29 | *OW5*[VII] (3.18(2) Å), OW7[VIII], *OW8* (3.09(1) Å) |
| O33 | N63[X] (2.92(1) Å), *OW6A*[I] (2.97(1) Å) | N34 | OP5[I] (2.92(1) Å), Cl[I] (3.248(9) Å), *OW10*[X] (2.62(1) Å) |
| O39 | **K1**[X] **(2.781(7) Å)** | N40 | N1CN (3.20(1) Å), *OW9*[XI] (3.02(1) Å), *OW15*[VIII] (3.12(1) Å) |
| O44 | OW4, *OW11*[XII] (2.89(1) Å), *OW15* (2.69(1) Å) | N45 | O28[X], OW7[XIII] |
| O51 | N63[XII] (3.08(1) Å), *OW5* (2.65(1) Å), *OW5A* (2.64(1) Å) | N52 | OW1[II], O28[XIV] |
| O58 | OW1[II] | N59 | Cl (3.086(8) Å) |
| O62 | **K1 (2.541(8) Å)** | N63 | O33[VI], O51[IX] |
| OR8 | **K1**[II] **(2.661(6) Å)**, *OW6*[II] (2.776(8) Å), *OW6A*[II] (2.773(8) Å) | OR8 | Cl[II] (3.178(7) Å) |
| OP4 | **K1**[II] **(2.877(6) Å)**, OW3[II] | OR7 | OW3 |
| OP5 | OW2, N34[II] | | |
| Cl | OW3, N34[II], N59, OR8[I] | | |

[a] Assignment of H-bonds involving the water molecules with full occupancy, the amide side chains, and the anions (if present) is given. Coordination bond lengths for cations are in boldface, while symbols of water molecules with fractional occupancy are in italics. [b] Operators for generating equivalent atoms: *I*, $x - 0.5, 0.5 - y, 1 - z$; *II*, $x + 0.5, 0.5 - y, 1 - z$; *III*, $1 + x, y, z$; *IV*, $x - 0.5, 0.5 - y, 1 - z$; *V*, $1 - x, y - 0.5, 0.5 - z$; *VI*, $-x, y - 0.5, 0.5 - z$; *VII*, $- x, 0.5 + y, 0.5 - z$; *VIII*, $1 - x, 0.5 + y, 0.5 - z$; *IX*, $1 - x, 0.5 + y, 0.5 - z$; *X*, $-x + 0.5, -y, z - 0.5$; XI, $x - 1, y, z$. [c] Operators for generating equivalent atoms: *I*, $x - 1, y, z$; *II*, $x - 0.5, 0.5 - y, 1 - z$; *III*, $0.5 + x, 0.5 - y, 1 - z$; *IV*, $1 + x, y, z$; *V*, $1.5 - x, -y, 0.5 + z$; *VI*, $0.5 - x, -y, 0.5 + z$; *VII*, $-x, 0.5 + y, 0.5 - z$; *VIII*, $-x, -0.5 + y, 0.5 - z$; *IX*, $0.5 - x, -y, z - 0.5$; *X*, $1 - x, 0.5 + y, 0.5 - z$; *XI*, $1.5 - x, -y, z - 0.5$. [d] Operators for generating equivalent atoms: *I*, $x - 0.5, 0.5 - y, 1 - z$; *II*, $x + 0.5, 0.5 - y, 1 - z$; *III*, $0.5 - x, -y, 0.5 + z$; *IV*, $x + 0.5, -0.5 - y, 1 - z$; *V*, $1.5 - x, -y, 0.5 + z$; *VI*, $-x, 0.5 + y, 0.5 - z$; *VII*, $x - 1, y, z$; *VIII*, $0.5 - x, -y, z - 0.5$; *IX*, $1 - x, 0.5 + y, 0.5 - z$; *X*, $-x, -0.5 + y, 0.5 - z$; *XI*, $x - 0.5, 0.5 - y, -z$; *XII*, $1 - x, y - 0.5, 0.5 - z$; *XIII*, $x - 0.5, -0.5 - y, 1 - z$; *XIV*, $1 + x, y, z$.

group positions in the case of the *b*, *c*, and *d* chains (only involved in H-bond with water molecules) are inverted with respect to the previous assignment in **4**.[4] It is likely that such differences between **1** and **4** are mostly due to the better resolution of the present structure determination, rather than to the presence of acetone molecules in the latter.

The crystal packing of **2** is very similar to that found in Cl- and $N_3$Cbl·2LiCl,[11,12] since it belongs to cluster IV, where all

**Chart 2**

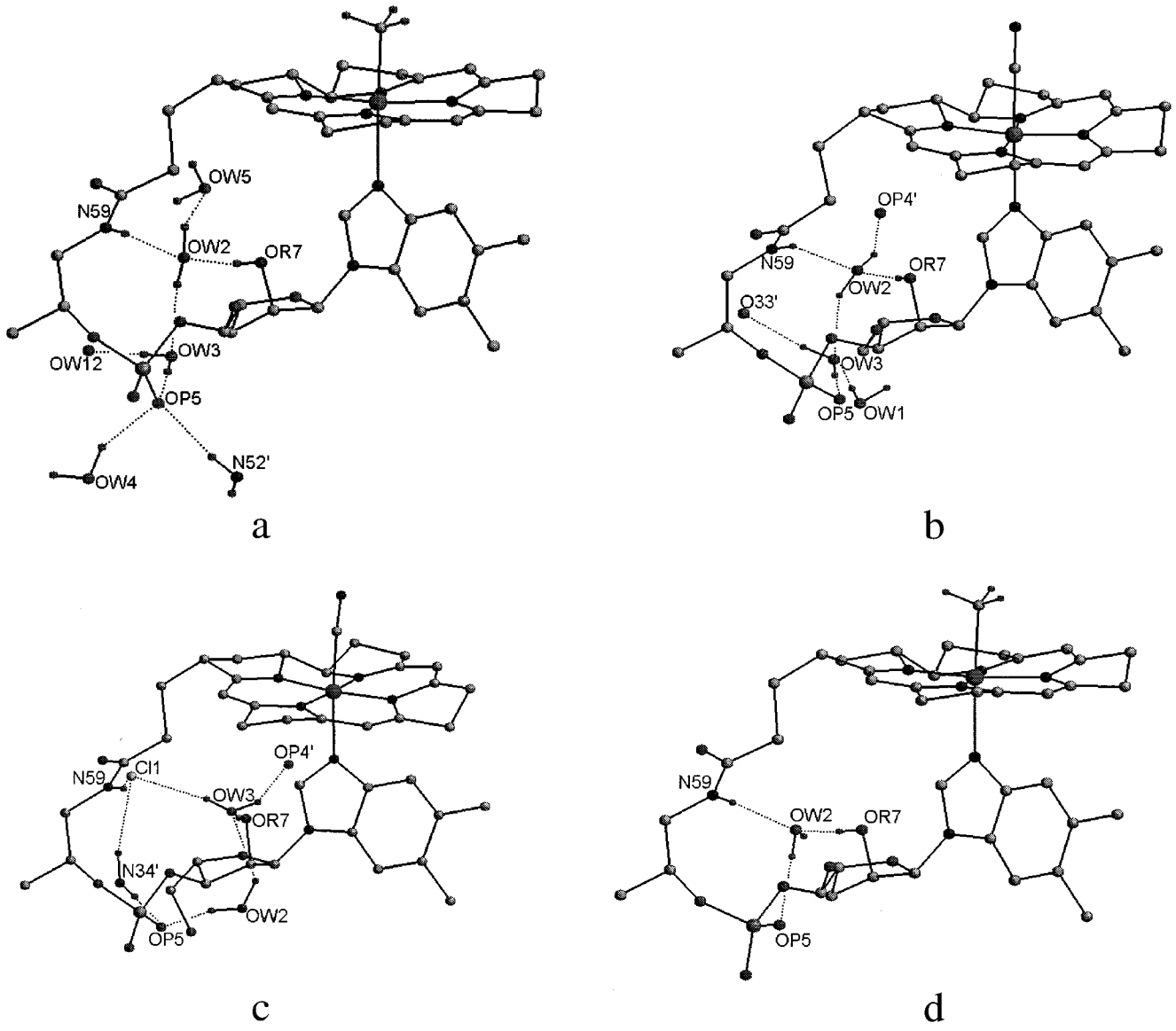


the amide chains have been found to interact with $Cl^-$ anions and water molecules through H-bonds and/or with $Li^+$ cations through amide O atom coordination. The only intermolecular H-bond between amide chains occurs between N29 (*a* chain) and O44 (*d* chain) at a distance of 3.270(5) Å. The H-bonding scheme including the water molecules with full occupancy is unequivocally assigned (Table 2). On the basis of the assignment of the H-bonds in Table 2, the structure inside the nucleotide loop is similar to that found in **1**, as shown in Chart 2b. The $Cl^-$ and $Li^+$ environments have been described previously.[11]

The crystal packing of **3** belongs to cluster I. Since the number of ions is halved and the water content is increased in the unit cell with respect to **2**, the diminished number of amide−ion interactions corresponds to an increase in the number of intermolecular H-bonds between the side chains. In fact, H-bond interactions between side chains (*a, e; a, d; e, g)* are found, in addition to those involving amide chains and water molecules (Table 2). Each $K^+$ ion is coordinated by O39 and O62 of two different cobalamin molecules and by OR8 and OP4 of the *f* chain of a single cobalamin molecule, in a distorted pyramidal arrangement with OP4 at the apex. The $Cl^-$ anion receives four H-bonds from OW3, N34, N59, and OR8. The two ions, bridged by OR8, make a short contact of 3.086(5) Å. The structure of the pocket in **3** is similar to that previously described[13] for $(SO_3$-Cbl$)(NH_4)$, in which $K^+$ replaces the ammonium ion, with the same environment of donors, and $Cl^-$ replaces a water molecule, which is instead H-bonded only to OW3, N59, and O62 in the sulfite cobalamin. This comparison gives an idea of the kind of local modifications which can occur within the pocket of two structures belonging to the same cluster, without appreciable influence on the overall packing. The structure inside the nucleotide loop is significantly different from those found in **1** and **2,** as can be seen by comparison of Chart 2c with Chart 2a and Chart 2b. In fact, N59 and OR7 are bridged by a $Cl^-$ ion and the water molecule OW3 (or by two water molecules in the other ion-free structures belonging to cluster I). However, as in **1** and **2** OW3 is H-bonded to OW2, which in turn donates a H-bond to OP5. The H-bonding pattern in the nucleotide loop of **3** (cluster I) is also detected in the structures of cluster II.[13]

**Molecular Structure of 1, 2, and 3.** The ORTEP drawings of **1**−**3** are shown in Figure 4. Visual comparison evidences that the thermal motion, particularly for the amide side chain atoms, decreases in the order **1** > **3** > **2**, corresponding to the increase in the number of ions per unit cell. The ions, interacting with amide chains, decrease the conformational freedom of the latter.

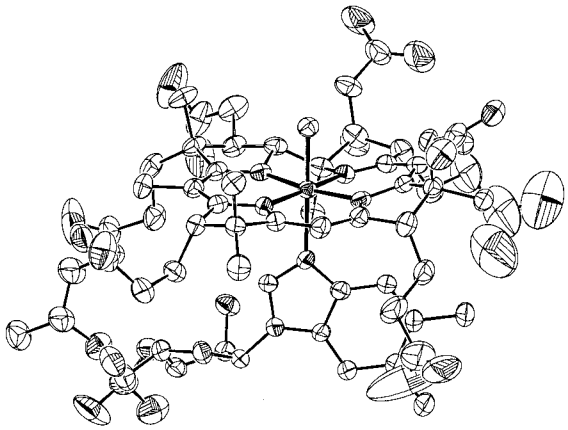

**1**

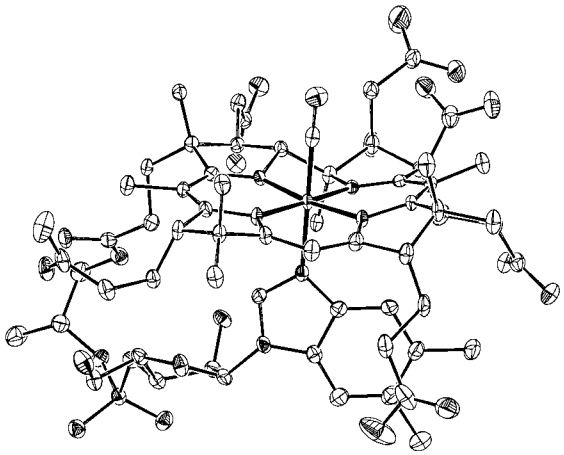

**2**

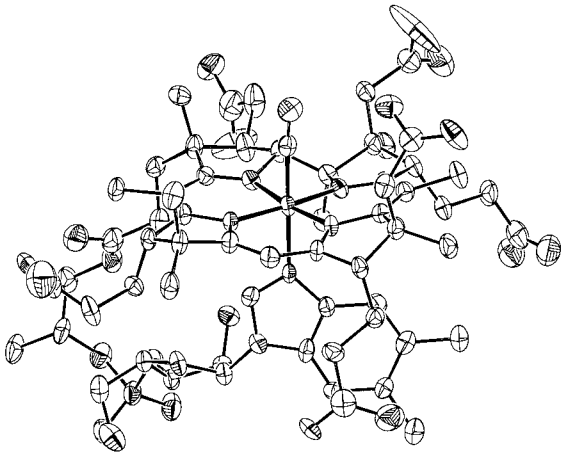

**3**

**Figure 4.** ORTEP drawings of **1**, **2**, and **3** with 50% probability thermal ellipsoids.

The folding angle, $\phi$, defined as the dihedral angle between the two planes passing through N21,C4,C5,C6,N22,C9,C10 and C10,C11,N23,C14,C15,C16,N24 is 14.7(2)°, 18.7(1)°, and 14.1(2)° in **1**, **2**, and **3**, respectively. The difference in $\phi$ between the cyanocobalamins **2** and **3** is surprising since it is close to the largest difference found in the known cobalamins.[20] On the other hand, the structural redetermination of the wet CNCbl, **5**,[22] which contains acetone solvent and belongs to cluster II, gave $\phi$ = 18.0(3)°. This aspect will be discussed in detail presently.

**Table 3.** Coordination Distances (Å) and Some Coordination Bond Angles (deg) in **1**, **2**, **3**, and **5** with Esd's in Parentheses

| | **1** (X = Me) | **2** (X = CN) | **3** (X = CN) | **5** (X = CN)[a] |
|---|---|---|---|---|
| Co−X | 1.979(4) | 1.886(4) | 1.868(8) | 1.86(1) |
| Co−NB3 | 2.162(4) | 2.041(3) | 2.029(6) | 2.01(1) |
| Co−N21 | 1.877(4) | 1.881(3) | 1.864(5) | 1.875(8) |
| Co−N22 | 1.922(4) | 1.911(3) | 1.904(5) | 1.908(8) |
| Co−N23 | 1.918(4) | 1.920(3) | 1.906(5) | 1.917(9) |
| Co−N24 | 1.874(4) | 1.883(3) | 1.896(5) | 1.875(8) |
| N21−Co−N22 | 89.6(2) | 90.0(1) | 90.7(2) | 90.4(4) |
| N21−Co−N24 | 83.3(2) | 83.5(1) | 83.2(2) | 83.8(4) |
| N22−Co−N23 | 96.7(2) | 95.8(1) | 96.2(2) | 96.8(4) |
| N23−Co−N24 | 90.6(2) | 90.9(1) | 89.9(2) | 89.2(4) |
| NB3−Co−X | 174.6(2) | 178.0(1) | 174.7(2) | 176.4(4) |

[a] Reference 22.

No intramolecular H-bond is found in **1**. As already observed[11] in cobalamins of cluster IV, two intramolecular H-bonds are found in **2**, one of 3.132(5) Å between N40 of the *c* chain and the nitrogen atom of the CN ligand; the other of 2.897(4) Å between OR8 (chain *f*) and O51 (chain *e*). Only the former kind of H-bond is found in **3** (3.20(1) Å), as occurs in cobalamins of cluster I. It should be noted that no intramolecular H-bond has been so far detected in structures of clusters II and III.[12]

The coordination distances in **1**−**3** and **5** are given in Table 3 and refer to the numbering scheme of Chart 1. The axial distances in **1** should be compared with those reported in **4** (Co−C = 1.99(2) Å and Co−NB3 = 2.19(2) Å).[9] Coordination distances in **2**, **3**, and **5** are very similar, within their respective experimental errors. The seemingly slightly shorter values in **3** and **5** could be related to the thermal $U_{eq}$ factor of the $CoCN_5$ grouping atoms, which are higher than those in **2**. Notwithstanding, the Co−N equatorial distances involved in the five-membered ring are shorter than the other two equatorial Co−N distances.[11−13] As expected, Me exerts a noticeably stronger trans influence than CN.

## Discussion

**Conformation of the Corrin Side Chains.** It has been reported that[12,13] the conformations of the amide side chains are similar for cobalamins belonging to the same cluster. The conformation of the chains in each cluster is defined on the basis of the sequence of the torsion angles along the amide chains, assuming that the conformations of a given chain are different when at least one torsion angle differs by more than 15°. The torsion angle, defining the amide group orientation, has not been considered in this scheme, since it covers a wide range of values. MeCbl and $(H_2OCbl)^+$ are assumed to be representative of "clusters" V and VI, respectively. Thus, the conformations of each chain are represented by the symbol of the chain, followed by a roman numeral subscript which defines a given conformation. With these assumptions, the scheme of Table 4 can be obtained. It is apparent that, excluding the orientation of the amide groups, chains *a* and *d* assume very similar conformations in all the structures, and chain *g* has essentially two conformations, while the others have a larger conformational freedom. It should be mentioned, however, that a few exceptions to the assignments of Table 4 may occur. For example, the conformation of the *c* chain in OHCbl, which belongs to cluster I,[12] is close to that of aquocobalamin, i.e., $c_{II}$ instead of $c_I$. This is easily explained by the similarity of the

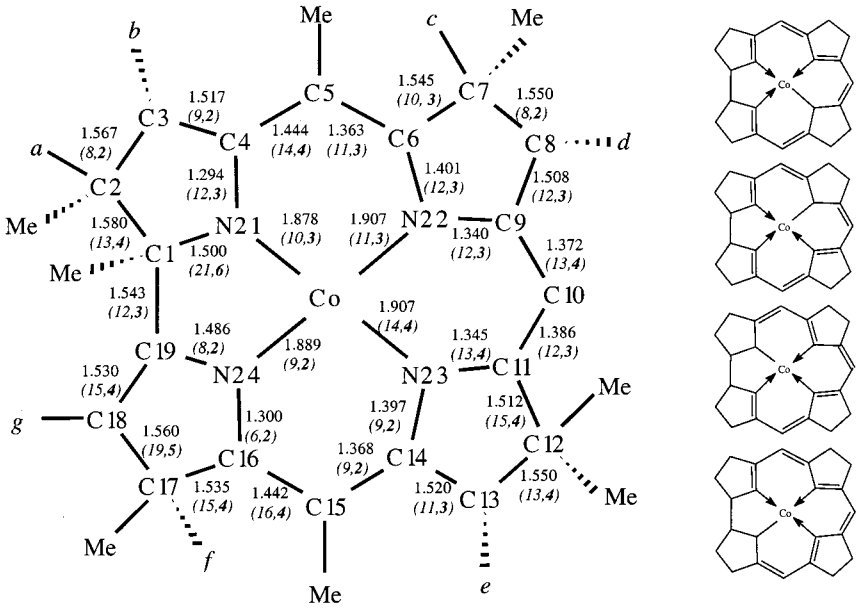


**Figure 5.** Mean bond lengths within the corrin nucleus. The first number in parentheses (lightface italic) represents the standard deviation of the sample, $\sigma = (\Sigma(x - x_m)^2/(n-1))^{1/2}$, the second (boldface italic) represents the standard deviation of the mean, $\sigma' = (\Sigma(x - x_m)^2/n(n-1))^{1/2}$. Four resonance structures for the delocalized corrin system are represented on the right side of the figure.

**Table 4.** Conformations of the Corrin Amide Side Chains in the Solid State

| cluster | conformation | | | | | | |
|---|---|---|---|---|---|---|---|
| I | $a_I$ | $b_{II}$ | $c_I$ | $d_I$ | $e_{II}$ | $f_{II}$ | $g_{II}$ |
| II | $a_I$ | $b_{II}$ | $c_{III}$ | $d_I$ | $e_{II}$ | $f_{II}$ | $g_{II}$ |
| III | $a_I$ | $b_{III}$ | $c_{III}$ | $d_I$ | $e_{III}$ | $f_{III}$ | $g_{II}$ |
| IV | $a_I$ | $b_I$ | $c_I$ | $d_I$ | $e_I$ | $f_I$ | $g_I$ |
| V | $a_I$ | $b_{IV}$ | $c_{III}$ | $d_I$ | $e_{II}$ | $f_{IV}$ | $g_{II}$ |
| VI | $a_I$ | $b_{II}$ | $c_{II}$ | $d_I$ | $e_{II}$ | $f_{II}$ | $g_I$ |

H-bond formation between the *c* chain and the axial ligand in the two cases. The conformational sequence in **1**, **2**, and **3** is close to that of MeCbl and of clusters IV and I of Table 4, respectively. The differences can be qualitatively appreciated by comparison of the corresponding ORTEP diagrams of Figure 4. It should be noted that in **1** the amido group plane of the *d* chain is approximately perpendicular to the benzimidazole plane, so that one of its H atoms points toward the center of the benzene ring. The same orientation of this amido group was observed only in the structure of the $B_{12}$ coenzyme, the other biologically active cobalamin.[15] Theoretical calculations suggested that such interaction results in an energy stabilization of 16.7 kcal/mol.[23]

**Geometry of the Corrin Nucleus.** As observed in the Introduction, molecular mechanics[7] and theoretical[8] calculations have been carried out in order to rationalize structural and electronic properties of cobalamins. Since it is likely that theoretical approaches, particularly those using the density functional method,[24] will be needed for a deeper understanding of the nature of the metal center, it is desirable that accurate geometrical parameters of this system are available. Some years ago, the mean values of bond lengths of the corrin nucleus were reported.[3] However the values were based on a limited number of structural determinations of low accuracy. Thanks to the present availability of accurate structural determinations, most of them based on synchrotron data, a more accurate analysis of the bond lengths within the corrin moiety can be now performed and the results rationalized in terms of electronic and steric factors. Eleven structural determinations based on synchrotron data (XCbl·2LiCl (X = CN, $N_3$,[11] Cl,[11] $NO_2$[12] at 100 K, X = $N_3$ and Cl at 275 K;[12] CNCbl·KCl at 100 K; $(H_2OCbl)(ClO_4)$ at 298 K;[9] OHCbl,[12] $(SO_3Cbl)(NH_4)$,[13] and $[(NH_2)_2CSCbl](PF_6)$[25] at 100 K) and two based on conventional X-ray sources ($O_2$Cbl·2LiCl at 96 K;[26] $HF_2$CCbl at 120 K[21]), with $R \leq 0.08$, were considered, and the corresponding distances within the corrin nucleus were averaged. The mean values, together with standard deviations, are given in Figure 5. The distances of the inner portion of the corrin ligand, which extends from N21 to N24 clockwise, are those expected for a conjugated system of C−C and C−N bonds: Furthermore, an approximately 2-fold symmetry with respect to the axis passing through Co and C10 (Chart 1) is apparent. Their trend can be qualitatively interpreted on the basis of the four resonance structures, sketched on the right side of Figure 5. The trend of the C−C single bond lengths, which vary from 1.508 Å (C8−C9) to 1.580 Å (C1−C2), reflects the different hybridization of the bonded C atoms as well as the number of their non-H substituents:

$$C_q{-}C_q > C_q{-}C_t > C_t{-}C_t \approx C_q{-}C(sp^2) > C_t{-}C(sp^2)$$

where $C_q$ and $C_t$ represent quaternary and tertiary C atoms, respectively. As already pointed out, the Co−N equatorial distances involved in the five-membered ring are shorter than the other two equatorial Co−N distances by about 0.020 Å.

The folding angle $\phi$ of the corrin moiety has been suggested[3] to reflect the bulk of the axial X ligand, decreasing with the increase of the latter.[5] However, more recently it has been observed[20] that $\phi$ decreases with the increase in the Co−NB3 distance, that is, with the increase in the trans influencing ability of X. An increase of about 0.3 Å corresponds to a decrease of about 5° in $\phi$ (Table 5). This has been attributed to the release of the steric pressure of the benzimidazole residue on the equatorial ligand. That the Co-$\beta$-cyano-imidazolylcobamide (the CNCbl analogue having the imidazole instead of the benzimi-

(23) Stasrikov, E. B.; Stener, T. *Acta Crystallogr.* **1998**, *B54*, 94.
(24) *Recent Developments and Applications of Modern Density Functional Theory*; Seminario, M., Ed.; Elsevier: Amsterdam, 1996.
(25) Toffoli, D. Thesis, University of Trieste, Italy, 1999.
(26) Hohenester, E.; Kratky, C.; Kräutler, B. *J. Am. Chem. Soc.* **1991**, *113*, 4523.

**Table 5.** Axial Distances (Å) in Cobalamins, Determined at Temperature *T* (deg), and in Cobaloximes at Room Temperature. The Folding Angle, $\phi$ (deg), for Cobalamins Is Also Reported

| | | XCbl | | | $XCo(DH)_2py$[a] | |
|---|---|---|---|---|---|---|
| X | *T* | C−X | Co−NB3 | $\phi$ | Co−X | Co−N(py) |
| $H_2O$ | room[b] | 1.952(2) | 1.925(2) | 18.7 | 1.916(3)[c] | 1.926(3)[c] |
| Cl | 100[d] | 2.252(1) | 1.981(3) | 17.9 | 2.229(1)[e] | 1.959(2)[e] |
| $NO_2$ | 100[f] | 1.896(5) | 1.989(5) | 16.7 | 1.943(3)[g] | 1.985(2)[g] |
| $N_3$ | 100[d] | 1.980(3) | 1.995(3) | 16.8 | 1.950(2) | 1.973(1) |
| CN | 88[h] | 1.858(10) | 2.011(10) | 18.0 | 1.937(2)[i] | 1.995(2)[i] |
| CN(KCl) | 100[j] | 1.868(8) | 2.029(6) | 14.1 | | |
| $(NH_2)CS$ | 100[k] | 2.300(2) | 2.032(5) | 14.8 | | |
| CN(LiCl) | 100[j] | 1.886(4) | 2.041(3) | 18.7 | | |
| $SO_3$ | 100[l] | 2.231(1) | 2.134(4) | 16.3 | 2.225(2)[l] | 2.042[m] |
| Me | 100[j] | 1.979(4) | 2.162(4) | 14.7 | 1.998(5) | 2.068(3) |
| $CHF_2$ | 120[n] | 1.949(8) | 2.187(7) | 15.6 | 1.948(5)[o] | 2.040[m] |
| Ado | 12[p] | 2.023(10) | 2.214(9) | 13.3 | 2.015(2)[q] | 2.072(2)[q] |

[a] Data from ref 5 if not otherwise stated. [b] Reference 9. [c] Attia, W. M.; Zangrando, E.; Randaccio, L.; Lopez, C. *Acta Crystallogr*. **1987**, *C43*, 1521. [d] Reference 11. [e] Geremia, S; Dreos, R.; Randaccio, L.; Tauzher, G.; Antolini, L. *Inorg. Chim. Acta* **1994**, *216*, 125. [f] Reference 12. [g] Unpublished results. [h] Reference 22. [i] Reference 30. [j] Present work. [k] Reference 25. [l] Reference 13. [m] Calculated values from ref 25 (see text). [n] Reference 21. [o] Reference 27. [p] Reference 15, Ado = 5-deoxy-5′-adenosyl. [q] Clegg, N.; Anderson, R. J.; Golding, B. T. *Acta Crystallogr*. **1989**, *C45*, 383; Ado = 5-deoxy-$\beta$-D-ribofuran-5-yl.

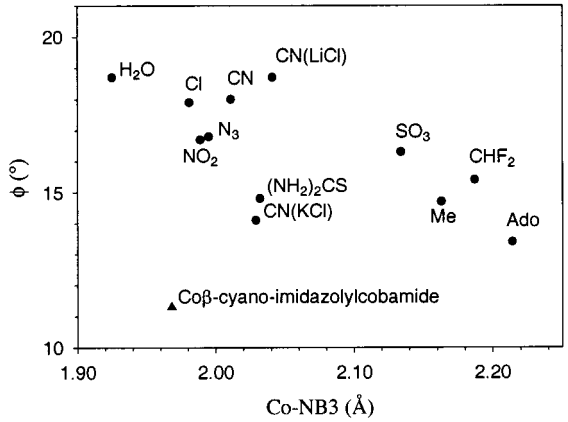


**Figure 6.** Plot of the folding angle $\phi$ against the Co−NB3 distance for cobalamins.

dazole residue in the *f* chain) does not fit the trend ($\phi$ = 11.3(2)° and Co−NB3 = 1.968(9) Å) was attributed to the smaller bulk of the imidazole than that of the benzimidazole residue.[20,22] The $\phi$ values for several cobalamins, including the imidazolyl derivative, determined with high accuracy, are given in Table 5, together with the Co−NB3 distances with esd's ≤ 0.01 Å. The trend of the Co−NB3 distance against $\phi$, given in Figure 6, confirms the previous observation. However, CNCbl·KCl and $[(NH_2)_2CSCbl](PF_6)$[25] do not follow the trend, the relative points being significantly shifted toward the imidazolyl side. This suggests that additional factors could influence the $\phi$ bending angle. However, it should be noted that the variations in $\phi$ amount to few degrees, suggesting that to a limited extent the *endogenous* wave deformation of the corrin moiety is affected by *exogenous* steric factors, induced by the axial ligands. If this is reasonable, some hypothesis about the factors affecting the homolysis in $B_{12}$ coenzyme should be reconsidered, although it is difficult to assess the effects that small variations in $\phi$ may have.

**Comparison between Cobalamins and Cobaloximes.** Available axial distances in cobalamins (with esd's ≤ 0.01 Å) and pyridine cobaloximes with L = py are given in Table 5. The py series was chosen because of the larger amount of data

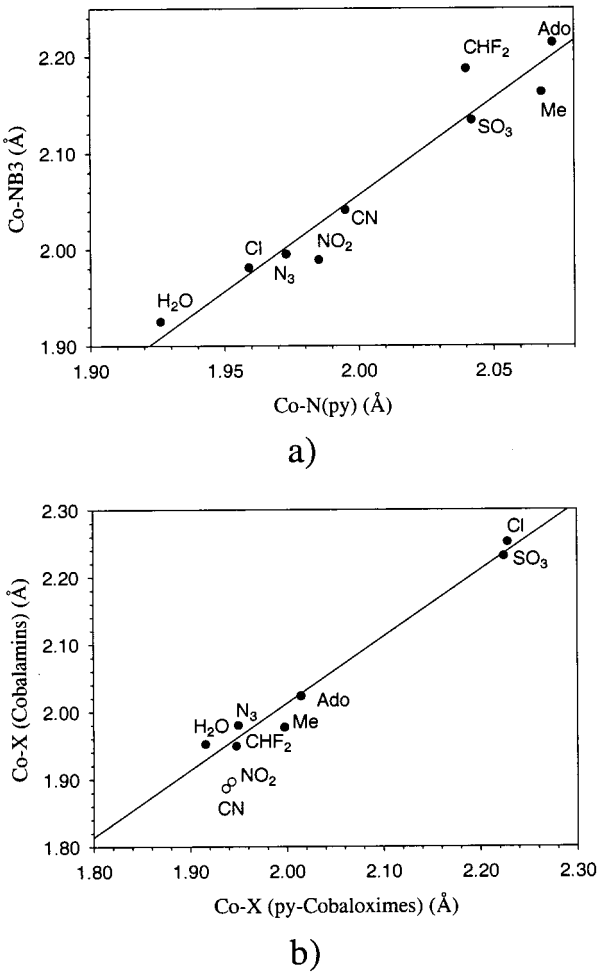


**Figure 7.** Plots of (a) the Co−NB3 distances against the Co−py distances in cobaloximes and (b) the Co−X distances in cobalamins against the analogous Co−X distances in cobaloximes.

available for comparison. This comparison should also be valid for cobaloximes with L= 1,5,6-trimethylbenzimidazole ($Me_3$-Bzm), since it has been shown[27] that the Co−C and Co−N distances are very similar for both the L ligands. The Co−py distances for X = $SO_3$ and $CHF_2$, experimentally not available, have been calculated accordingly to refs 13 and 25.

We have previously shown[13] that there is a good linear relationship between Co−py and Co−NB3 distances, when X = $H_2O$, Cl, $N_3$, CN, Me, and Ado. This comparison indicated a greater sensitivity of the Co−NB3 bond length relative to that of Co−py in responding to the trans influence of X. When data for X = $CHF_2$, $SO_3$, and $NO_2$ were included, the previous relationship was confirmed and the relative linear regression gave $r^2$ = 0.938 with a slope of 2.00(19) (Figure 7a).This indicated that the cis influence of the corrin nucleus is noticeably greater than that of the $(DH)_2$ one. Since the Co−NB3 distances in aquocobalamin and cobaloxime are very close, the cis influence is predominantly electronic, despite the more crowded corrin ring (see below). It should be noted that the Co−NB3 distance in $CHF_2$Cbl is slightly longer than that of MeCbl. This is unexpected[18] since fluoroalkyl derivatives should have a trans influence significantly less than that of the analogous alkyls, as shown in simple $B_{12}$ models.[28] On the other hand, the Co−

(27) Randaccio, L.; Geremia, S.; Zangrando, E.; Ebert, C. *Inorg. Chem.* **1994**, *33*, 4641 and references therein.
(28) Geremia, S.; Randaccio, L.; Zangrando, E. *Gazz. Chim. Ital.* **1992**, *122*, 229.

$CHF_2$ bond is shorter (0.03 Å) than the Co−Me bond, as found in cobaloximes. The shortening has been attributed to the greater electron-withdrawing ability of fluoroalkyl than that of the corresponding alkyl group.[28]

The plot of the Co−X distances in cobalamins and cobaloximes is reported in Figure 7b. The regression gave the equation

$$\text{Co−X(Cbl)} = [0.988(64)]\text{Co−X(cobaloxime)} + 0.04(13),\ r^2 = 0.979,\ n = 7$$

if the CN and $NO_2$ groups were excluded. When the latter were included the equation was Co−X = [1.069(94)]Co−X − 0.14(19), and $r^2 = 0.949$ (only the more accurate value for CNCbl in **2** is considered). This appears to indicate that the Co−X distances are very similar in cobalamins and in cobaloximes.[29] However, those relative to CN and $NO_2$ groups fall significantly *below* the values predicted by the correlation for the other groups. This suggests strongly that the $\pi$-back-electron-donation from Co to CN (and possibly to $NO_2$), shown to be appreciable in these systems by Brown et al. by means of $^{15}N$ and $^{13}C$ NMR measurements,[30] is more enhanced in cyanocobalamins than in cyanocobaloximes. Such a difference can be structurally measured by the shortening of about 0.05 Å of the Co−C bond and by the lengthening of about 0.09 Å of the C−N bond (from 1.077(3) Å[31] to 1.164(6) Å) in the cyanocobalamin with respect to the cyanocobaloxime. Comparison of $^{15}N$ and $^{13}C$ resonances of the CN group in cobalamins[30a] and cobaloximes[30b] supports this suggestion. In CNCbl, the $^{15}N$ resonance is about 20 ppm shifted upfield and the $^{13}C$ resonance about 7 ppm shifted downfield with respect to those in $(CN)Co(DH)_2L$, with L = py, whose $pK_a$ is close to that of $M_3Bzm$ (cis influence). This is in agreement with an increase in the electron $\pi$-donation from Co to the CN group.[30] Analogously, the $\nu_{C\equiv N}$ in CNCbl is 2141.0 $cm^{-1}$ [30c] whereas it is 2132.0 $cm^{-1}$ in the $CNCo(DH)_2py$.[30b] These structural and spectroscopic findings could represent a quantitative measure of the different behavior of the cobalt center in the two systems, due to the greater electronic charge put on the metal center by the corrin ligand as compared to that of dimethylglyoximates. Available electrochemical data nicely agree with this view. In fact, the one electron reduction potential for MeCbl was reported to be −1.60 V by Lexa and Saveant.[32] This value was confirmed by a subsequent work,[33] which also reported a value of −1.38 V for neopentylcobalamin. The $E_{1/2}$ values for $XCo(DH)_2(Me_3Bzm)$, with X = Me and neopentyl, are −1.45 V and −1.27 V, respectively,[34] remarkably shifted toward less negative values with respect to cobalamins. Therefore, it may be concluded that the greater electron richness of Co in cobalamins, on one hand, enhances the back-donation to CN with respect to cobaloximes and, on the other, makes the transmission of the trans influence more effective in cobalamins.

It has been reported[35] that axial Co−NB3 distances are well correlated with several magnetic resonance parameters of some cobalamins (X = $H_2O$, CN, Me, ade (5-adenylpropyl), Ado). Particularly, the $^{31}P$ shifts were suggested to be a reliable tool of estimating the Co−NB3 bond lengths,[35] despite their relatively small variation across the series. In fact, the $^{31}P$ shifts/Co−NB3 distance correlation gives an $r^2$ correlation factor of 0.997. However, when $^{31}P$ chemical shifts, reported[36] for a more extended series of cobalamins (with X = $H_2O$, OH, $N_3$, CN, $CHF_2$, Me, Ado), are correlated with the Co−NB3 distance given in Table 5, the correlation factor drops to 0.900.

**Comparison of the Solution and Solid-State Structures of MeCbl.** Some years ago, an NMR study of MeCbl and other cobalamins in water solution proved that the NMR technique is useful in assessing conformational and structural changes in cobalamins.[4] Recently, a comparison of the structure in solution of MeCbl, determined by NMR spectroscopy, with that of **4** has been reported.[37] Similarities and differences which concern the conformation of the side chains were found. Thus, in solution the *a* and *d* chains (Chart 1) were found to have a notable conformational rigidity, whereas the *b*, *c*, *e*, and *g* chains were conformationally flexible to different extents. This result corresponds nicely with that derived from the qualitative conformational analysis of the chains previously illustrated (Table 4), and it is also supported by the detailed description of the internal motions of MeCbl and CNCbl in solution by NMR-restrained modeling.[38] Previous comparison[37] of the solution and solid-state structure in **4** has underlined several conformational differences within the nucleotide loop.[37] Some of these can be now removed by some incorrect assignments due to the scarcely accurate structure of **4**. Actually, when comparison is made with **1** the only significant difference within the nucleotide loop in solution and in the solid state concerns the OW2 molecule (compare Chart 2a and Chart 2d). This molecule, which bridges N59 and OR7, receiving two H-bonds in both cases, donates a H-bond to OP5 in solution. On the contrary, in the solid state OW2 gives the H-bond to OW3, which in turn donates a H-bond to OP5 (see crystal packing section). On the other hand, the H-bonding scheme within the nucleotide loop of **1** is very similar to that in CNCbl·2LiCl (Chart 2b) and in all the other "inorganic" cobalamins of cluster IV, where the H-bond assignment was unequivocally determined, as shown in the crystal packing section. In CNCbl·KCl, as well as in $(SO_3Cbl)(NH_4)$[13] and $[(NH_2)_2CSCbl](PF_6)$[25] (and probably in all cobalamins belonging to clusters I and II), N59 and OR7 are, in addition, far apart, with a bridge made by OW3 and Cl (or by two water molecules) (Chart 2c).

The difference in the H-bonding scheme within the nucleotide loops between solution and solid states may be related to the different values of the torsion angle $\epsilon$, namely, CR2−CR3−OP2−P (Chart 1). In fact, from NMR measurements in solution this angle was evaluated to be close to 90°,[37] whereas in **1** it is 120.9(4)°. The former value could bring OP5 closer to OW2 at a distance suitable for H-bond formation, while in **1** the OW2···OP5 distance is 4.10 Å. However, in **2**, which exhibits a H-bonding scheme very similar to that of **1** (compare Chart 2a

(29) It should be recalled that data collected at low temperature could imply slightly longer distances. However, it has been shown[12] that coordination distances (but not those of the side chains) in cobalamins do not significantly differ in Cl- and $N_3$Cbl, when data are collected at 100 and 275 K.

(30) (a) Brown, K. L.; Gupta, B. D. *Inorg. Chem.* **1990**, *29*, 3854. (b) Brown, K. L.; Satyanarayana, S. *Inorg. Chem.* **1992**, *31*, 1366. (c) Pratt, J. M. In *Chemistry and Biochemistry of $B_{12}$*; Banerjee, R., Ed.; J. Wiley & Sons: New York, 1999; p 73.
(31) Attia, W. M.; Zangrando, E.; Randaccio, L.; Antolini, L.; Lopez, C. *Acta Crystallogr.* **1989**, *C45*, 1500.
(32) Lexa, D.; Saveant, J. M. *J. Am. Chem. Soc.* **1978**, *100*, 3220.
(33) Sheperd, R. E.; Zhang, S.; Dowd, P.; Choi, G.; Wick, B.; Choi, S. *Inorg. Chim. Acta* **1990**, *174*, 249.
(34) Peressini, S. Private communication.
(35) Brown, K. L.; Evans, D. R.; Zubkowski, J. D.; Valente, E. J. *Inorg. Chem.* **1996**, *35*, 415. Xou, X.; Brown, K. L. *Inorg. Chim. Acta* **1998**, *267*, 305.
(36) Calafat, A. M.; Marzilli, L. G. *J. Am. Chem. Soc.* **1993**, *115*, 9182.
(37) Konrat, R.; Tollinger, M.; Kräutler, B. In *Vitamin $B_{12}$ and $B_{12}$-Proteins*; Kräutler, B., Arigoni, D., Golding, B. T., Eds.; Wiley-VCH: Weinheim, 1998; p 349. Tollinger, M.; Konrat, R.; Kräutler, B. *Helv. Chim. Acta* **1999**, *82*, 158.
(38) Brown, K. L.; Marques, H. M. *J. Mol. Struct. (THEOCHEM)* **1998**, *453*, 209.

and Chart 2b), the $\epsilon$ angle is 100.6(3)° close to that evaluated in solution, but still the OW2···OP5 distance is 3.56 Å. On the other hand, changes of about 15° in the torsion angles around N59−CPr1 and OP3−P bonds occur, the other torsion angles along the *f* chain between C56 and P being essentially constant with respect to **1**. It can be recalled that in AdoCbl a water molecule still bridges N59 and OR7, but it donates a bifurcated H-bond to OR7 and OP2, with a distance to OP5 of 4.14 Å. Therefore, no direct H-bond between OP5 and the water molecule bridging N59 and OR7 (Chart 2d) has been detected so far in the solid state.[37]

**Acknowledgment.** We thank Ministero della Ricerca Scientifica e Tecnologica (Roma) (PRIN 9803184222) and Consiglio Nazionale delle Ricerche (CNR) for financial support. Thanks are due to the CNR staff at Elettra, Trieste, Italy, for helping at the Crystallographic Beamline, supported by CNR and Sincrotrone Trieste.

**Supporting Information Available:** Three X-ray crystallographic files, in CIF format, are available. This material is available free of charge via the Internet at http://pubs.acs.org.

IC0001199